ground water

The Geochemical Evolution of Riparian Ground Water in a Forested Piedmont Catchment

by Douglas A. Burns[1,2], L. Niel Plummer[3], Jeffrey J. McDonnell[1,4], Eurybiades Busenberg[3], Gerolamo C. Casile[3], Carol Kendall[5], Richard P. Hooper[6,7], James E. Freer[1,8], Norman E. Peters[6], Keith Beven[8], and Peter Schlosser[9]

Abstract

The principal weathering reactions and their rates in riparian ground water were determined at the Panola Mountain Research Watershed (PMRW) near Atlanta, Georgia. Concentrations of major solutes were measured in ground water samples from 19 shallow wells completed in the riparian (saprolite) aquifer and in one borehole completed in granite, and the apparent age of each sample was calculated from chloroflourocarbons and tritium/helium–3 data. Concentrations of SiO_2, Na^+, and Ca^{2+} generally increased downvalley and were highest in the borehole near the watershed outlet. Strong positive correlations were found between the concentrations of these solutes and the apparent age of ground water that was modern (zero to one year) in the headwaters, six to seven years midway down the valley, and 26 to 27 years in the borehole, located ~500 m downstream from the headwaters. Mass-balance modeling of chemical evolution showed that the downstream changes in ground water chemistry could be largely explained by weathering of plagioclase to kaolinite, with possible contributions from weathering of K-feldspar, biotite, hornblende, and calcite. The in situ rates of weathering reactions were estimated by combining the ground water age dates with geochemical mass-balance modeling results. The weathering rate was highest for plagioclase (~6.4 µmol/L/year), but could not be easily compared with most other published results for feldspar weathering at PMRW and elsewhere because the mineral-surface area to which ground water was exposed during geochemical evolution could not be estimated. However, a preliminary estimate of the mineral-surface area that would have contacted the ground water to provide the observed solute concentrations suggests that the plagioclase weathering rate calculated in this study is similar to the rate calculated in a previous study at PMRW, and three to four orders of magnitude slower than those published in previous laboratory studies of feldspar weathering. An accurate model of the geochemical evolution of riparian ground water is necessary to accurately model the geochemical evolution of stream water at PMRW.

Introduction

The development of conceptual and mathematical models of hydrologic and biogeochemical processes in small watersheds has been largely based on observations from hillslope soils (Cosby et al. 1985; Reuss and Johnson 1986; Johnson and Lindberg 1992). The importance of hillslopes is supported by hydrologic data in which a coincident response of the water table on hillslopes and streamflow in the adjacent valley has been observed (Wheater et al. 1991; Turton et al. 1992). Nevertheless, recent work has shown little expression of hillslope water chemistry in stream water, even during rain events (Burns et al. 2001). Consequently, riparian or near-stream ground water is hypothesized to be the dominant control of stream water chemistry in many small watersheds, especially during base flow and even during high flow (Bishop et al. 1990; Robson et al. 1992; Peters and Ratcliffe 1998; Burns et al. 2001). Riparian aquifers serve as reservoirs that can store ground water for months or years, while sustaining stream base flow. The rapid rise of potentiometric head in riparian aquifers in response to rain events causes the release of a large volume of ground water to the stream, although the physical mechanism underlying such a rapid

[1]State University of New York, College of Environmental Science and Forestry, Syracuse, New York
[2]U.S. Geological Survey, Troy, New York
[3]U.S. Geological Survey, Reston, Virginia
[4]Oregon State University, Corvallis, Oregon
[5]U.S. Geological Survey, Menlo Park, California
[6]U.S. Geological Survey, Atlanta, Georgia
[7]U.S. Geological Survey, Northborough, Massachusetts
[8]University of Lancaster, Lancaster, U.K.
[9]Lamont-Doherty Earth Observatory and Department of Earth and Environmental Engineering, Columbia University, New York

rise in head is subject to debate (Jayatilaka and Gillham 1996; Gillham and Jayatilaka 1998; McDonnell and Buttle 1998).

Two recent studies at the Panola Mountain Research Watershed (PMRW) in the Piedmont region of Georgia indicated the dominance of riparian ground water rather than hillslope ground water in that: (1) the chemistry of riparian ground water differs from that of hillslope ground water and soil water—an indication that the relative importance of biogeochemical processes that control the chemistry of these waters differ (Hooper et al. 1998), and (2) riparian ground water, rather than hillslope ground water, dominates base flow and also forms a large percentage of stream flow during rainstorms (Burns et al. 2001).Thus, the development of accurate models of stream water chemistry at PMRW will require a correct understanding of the principal biogeochemical processes and their rates in the riparian aquifer.

The concentrations of major solutes in ground water at a series of riparian-aquifer wells adjacent to the stream at PMRW were used to develop a mass-balance model of the principal weathering reactions that affect the chemical evolution of riparian ground water. Chlorofluorocarbon (CFC) and tritium/helium–3 ($^3H/^3He$) tracer data were then used to calculate the apparent age of each riparian ground water sample. Strong correlations between the apparent ages and concentrations of Na^+, Ca^{2+}, and SiO_2 were then used to estimate the mean apparent age of stream water. Finally, geochemical mass-balance modeling results were combined with the apparent ground water ages to calculate rates of chemical weathering in the riparian aquifer. This method is similar to an approach previously published by Rademacher et al. (2001) to calculate weathering rates in 11 springs in the Sierra Nevada Mountains of California. Linking age-dating techniques with riparian ground water chemistry to calculate in situ rates of biogeochemical processes provides an approach that may lead to a new generation of stream-chemistry models that reflect the central role and distinct nature of riparian ground water in small watersheds such as the PMRW.

Study Site

The PMRW (41 ha) is located in the southern Piedmont province of Georgia, ~25 km southeast of Atlanta (Figure 1). The watershed is forested (except for extensive granite outcrops) by hickory, oak, tulip poplar, and loblolly pine (Carter 1978), and is underlain by the Panola Granite, which is intruded into the Clairmont Formation (Higgins et al. 1988). The Panola Granite is a biotite-oligoclase-quartz-microcline granite of Mississippian to Pennsylvanian age (Atkins and Higgins 1980). The Clairmont Formation is a melange containing variable amounts of amphibolite, granite gneiss, and other rock types of Ordovician age (Higgins et al. 1988). The weathering of amphibole minerals such as hornblende in the Clairmont Formation may provide greater amounts of Mg^{2+} to drainage waters than the weathering of Panola Granite. The watershed contains no outcrops of the Clairmont Formation, but drilling has found pods and lenses of it in the lower part of the watershed (Huntington et al. 1993). The upper part of the watershed

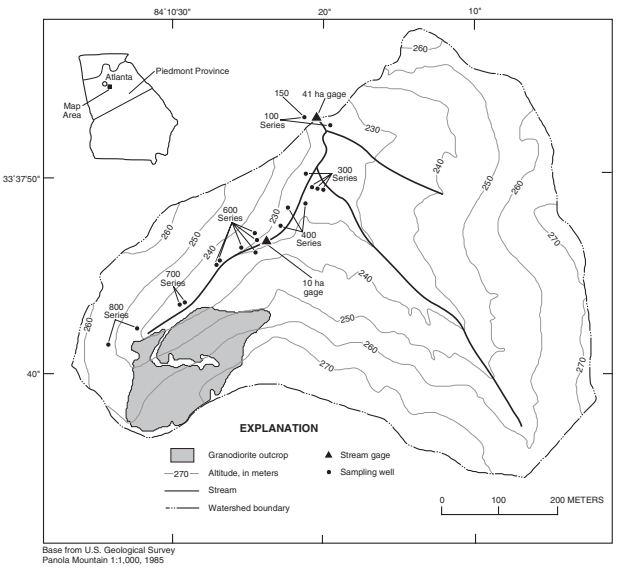

Figure 1. Locations of streamflow gauges and wells sampled during March 10–15, 1996, at Panola Mountain Research Watershed, Georgia.

contains a 3.6 ha outcrop of Panola Granite, upstream (SW) of a 10 ha drainage area gage nested within the 41 ha watershed (Figure 1).

The primary minerals in the Panola Granite are plagioclase feldspar, quartz, microcline/microperthite, biotite, and muscovite (Grant 1975; Kelly 1987; White et al. 2001). Much of the Clairmont Formation has similar mineralogy to that of the Panola Granite, except for the amphibolite lenses found in bedrock drill cores in the lower part of the watershed. This amphibolite is dominated by hornblende and plagioclase feldspar with minor amounts of quartz, epidote, and hematite (Kelly 1987). The plagioclase in the Panola Granite has a composition of $An_{20–25}$ (20% to 25% calcic and 75% to 80% sodic), whereas the plagioclase in the amphibolite is more calcic, with a mean composition of An_{32} (Kelly 1987; White et al. 2001).

The dominant secondary minerals are kaolinite (and halloysite), hydroxy-interlayered vermiculite, hydrobiotite, gibbsite, and goethite (Nixon 1981; Shanley 1989; White et al. 2001). Weathering studies of the surface of the granite outcrop and of soils indicate that the dissolution of plagioclase is the dominant weathering reaction at PMRW (Nixon 1981; White et al. 2001). Plagioclase weathers in the soils and saprolite to kaolinite; K-feldspar and biotite also show evidence of weathering to kaolinite (White et al. 2001). Biotite weathers to vermiculite, as supported by electron backscatter images and electron microprobe examination of regolith (White et al. 2001). Biotite weathers more rapidly than muscovite, as indicated by soil samples that show little weathering of the muscovite, but almost complete removal of biotite (White et al. 2001).

The soils at PMRW are predominantly red, clay-rich Ultisols formed by weathering of the Panola Granite. These soils are developed on alluvium and colluvium and grade to Inceptisols in the colluvium, in recent alluvium, or in eroded areas (Huntington et al. 1993). Soils are generally from 0.5 to 1.5 m thick and overlie saprolite of variable thickness.

The climate at PMRW is classified as humid, subtropical; mean annual temperature is 16.3°C, and mean annual precipitation is 1240 mm (National Oceanic and Atmospheric Administration 1991). Streamflow at PMRW has a strong seasonal pattern, with the highest flow from October through March, and the lowest flow from April through September. Evapotranspiration represents ~70% of annual rainfall in this region of the United States (Carter and Stiles 1983).

Streamflow at PMRW is monitored by compound 90° v-notch weirs at the outlet of the watershed and upstream at a site that monitors the southwest quarter of the watershed. Stream water chemistry from both of these gauges is discussed in this paper.

The Panola watershed is notable for the sharp contrast between the chemistry of riparian ground water, which is dominated by Na^+ and HCO_3^-, and the chemistry of hillslope ground water, which is dominated by Ca^{2+} and SO_4^{2-}(Hooper et al. 1998). The riparian area, which is underlain by the riparian aquifer, occupies 8% of the 10 ha watershed, and the average depth to bedrock is 3.57 m, whereas hillslopes occupy 57% of the watershed, and the average depth to bedrock is 1.18 m (Zumbuhl 1999; Burns et al. 2001). The riparian area was assumed to occupy the stream valley and extend up the hillslopes until the depth to bedrock was <3 m, similar to previous studies (Burns et al. 2001).

Methods

Ground water and surface water samples were collected for analysis of major chemical constituents, and CFC and $^3H/^3He$ tracers. A geochemical mass-balance model was used to describe the principal chemical weathering reactions that influence the geochemical evolution of riparian ground water.

Field Procedures

Ground water and stream water samples were collected for chemical, CFC, and $^3H/^3He$ analyses at base flow conditions during March 10–15, 1996. Samples for chemical analysis were collected in 250 mL polyethylene bottles. Stream water was collected with a peristaltic pump at the two gauges. Ground water was collected from 19 wells and a borehole (Figure 1) by either a Bennett or peristaltic pump. The pH of each ground water sample was measured with an electrode and pH meter in the field. All wells were purged to flush at least three well volumes prior to sampling. The Bennett pump was fitted with nylon and copper discharge lines, and the peristaltic pump was fitted with a copper line to minimize contamination of samples for CFC analysis. Samples for CFC analysis were collected by a system that eliminates air-water contact during sampling (Busenberg and Plummer 1992). Water samples were flame sealed into borosilicate glass ampoules without allowing air contact. Samples for ^3H analysis were collected in 500 mL polyethylene bottles, and samples for helium and neon analysis were collected under back pressure in 10 mm O.D. copper tubes with pinch-off clamps.

Most wells consist of 51 mm O.D. PVC casing with screen lengths that range from 0.3 to 1.52 m; well 150 (Figure 1) consists of 101.6 mm OD PVC pipe that extends from the surface to bedrock, below which is an open borehole to a depth of 19.8 m below the surface. The depth of the midpoint of the well screens range from 1.13 to 4.27 m. Most wells are completed in saprolite; well 150 is completed in Panola Granite. Some wells in the 300 and 600 series (322, 323, 324, 671.261, and 671.373) are nested, each with short screen lengths of 0.3 m to allow study of changes of ground water age and chemistry with depth.

Laboratory Procedures

Ground water and stream water samples for chemical analysis were passed through 0.45 µm cellulose acetate filters. A sample aliquot was acidified to a pH < 2 with concentrated HNO_3 prior to analysis for base cations and silica. All samples were stored at room temperature prior to analysis of Ca^{2+}, Mg^{2+}, Na^+, K^+, Sr^{2+}, and SiO_2 concentrations by direct-current plasma emission spectroscopy, Cl^- and SO_4^{2-} concentrations by ion chromatography, and alkalinities by Gran titration. The pH of each stream sample was determined with an electrode and pH meter. The relative precision of duplicate samples (10% of samples analyzed) was ±5% for base cation and SiO_2 concentrations and ±3% for Cl^- concentrations, based on analyses during the year prior to and including the analysis dates for this study. Five ampoules were collected at each well and sealed in the field, and three of these were analyzed for CFCs (CFC–11, CFC–12, CFC–113) by purge-and-trap gas chromatography according to methods described by Busenberg and Plummer (1992). The reported concentration for each CFC species is the mean of three analyses. Samples were also analyzed for O_2, N_2, Ar, CO_2, and CH_4 by gas chromatography.

Henry's law and solubility data (Warner and Weiss 1985; Bu and Warner 1995) were used to convert the measured CFC concentrations in water to the gas partial pressures (in parts per trillion by volume, pptv) that would be in air in equilibrium with each sample at the recharge temperature determined from the N_2–Ar data (Heaton 1981; Heaton and Vogel 1981). The recharge date was determined by comparing the derived CFC partial pressures to the historical CFC concentrations in North American air (Plummer and Busenberg 2000; *http://water.usgs.gov/lab/cfc*). The apparent age is simply the difference between sample date and recharge date. Four air samples were collected during the sampling period, and their CFC concentrations were close to that of North American clean air for 1996, except for CFC–11 concentrations that were slightly higher, possibly due to local contamination from the surrounding Atlanta metropolitan area. Most of the recharge temperature values range from 8° to 14°C, considerably lower than the mean annual air temperature of 16.3°C, suggesting that most ground water recharge at PMRW occurs during winter. Many of the ground water temperature measurements also fell within the 8° to 14°C range (Table 1).

Ground water samples for ^3H were analyzed at the Lamont-Doherty Earth Observatory Noble Gas Laboratory. Water samples were degassed quantitatively using a vacuum-extraction system. Helium and neon were purified and separated from each other by a cryogenic cold trap in the inlet system of the dedicated helium isotope mass spectrometer. The ^4He concentrations and $^3He/^4He$ ratios were

Table 1
Water-Sampling Dates, Well Depths, Water Temperature, and Concentrations of Selected Dissolved Constituents in Samples from Wells and Stream Sites at Panola Mountain Research Watershed, Georgia, March 10–15, 1996

Sampling Site	Date	Well Depth (m)	Water Temp. (°C)	Concentrations (mg/L)									
				Ca^{2+}	Mg^{2+}	Na^{+}	K^{+}	Sr^{2+}	Cl^{-}	SO_4^{2-}	SiO_2	pH	(HCO_3^{-})
Wells													
130	3/11/96	1.4	16.5	1.07	0.59	2.93	0.61	0.012	1.39	1.41	14.8	6.29	11.8
150	3/11/96	19.8	15.4	5.12	0.84	7.37	1.33	0.043	2.10	0.74	38.1	6.20	35.5
285	3/15/96	3.6	16.1	0.39	0.96	0.66	2.12	0.009	1.33	4.95	4.2	5.26	4.7
316	3/12/96	1.6	13.5	1.74	0.90	2.02	0.77	0.011	1.61	2.83	10.6	6.08	10.8
322	3/11/96	1.1	8.5	1.18	0.73	1.82	1.00	0.009	1.65	3.76	8.4	6.51	6.7
323	3/12/96	1.4	9.8	2.08	1.16	2.72	0.73	0.013	1.63	1.20	14.6	5.95	18.5
324	3/12/96	1.7	10.9	2.10	1.16	2.86	0.68	0.013	1.63	0.99	15.8	6.01	17.2
418	3/12/96	0.9	13.3	2.27	0.80	4.07	1.03	0.017	1.82	0.37	20.9	5.15	19.6
441	3/15/96	3.4	14.4	0.88	0.57	1.48	1.21	0.011	1.89	1.16	7.6	5.68	7.5
479	3/15/96	3.4	14.1	0.11	0.30	1.92	0.67	0.003	2.39	<0.5	10.1	5.17	5.7
640	3/12/96	2.9	12.0	0.81	0.25	1.79	0.30	0.007	1.28	2.58	7.9	5.35	4.3
671.261	3/14/96	2.6	15.8	0.84	0.28	1.86	0.46	0.006	1.31	2.44	8.8	5.17	4.7
671.373	3/14/96	3.7	19.5	0.83	0.28	1.97	0.38	0.007	1.29	2.32	8.8	5.37	6.9
690	3/13/96	2.1	12.6	0.84	0.30	1.55	0.41	0.008	1.27	3.20	6.7	6.02	2.9
691	3/13/96	4.3	12.4	0.91	0.34	1.71	0.39	0.009	1.30	2.81	8.4	5.36	3.8
696	3/13/96	3.4	12.2	0.86	0.30	1.43	0.38	0.008	1.10	3.55	6.3	5.20	2.0
737	3/13/96	1.1	17.2	0.43	0.16	0.81	0.12	0.006	0.86	5.40	3.9	4.35	0.0
760	3/13/96	1.7	15.2	0.53	0.26	1.07	0.16	0.007	1.19	4.82	4.4	5.09	1.6
801	3/14/96	3.3	12.2	0.71	0.46	2.35	0.50	0.008	1.66	3.69	9.7	5.08	4.4
821	3/14/96	na	12.0	0.55	0.74	1.09	1.05	0.007	1.47	4.03	5.5	5.11	3.5
Stream Sites													
100 (41 ha gauge)	3/11/96		11.8	1.12	0.54	2.14	0.80	0.010	1.48	1.81	10.7	6.30	7.9
100	3/15/96		14.3	1.14	0.57	2.23	0.83	0.009	1.59	1.57	11.2	6.30	8.9
601 (10 ha gauge)	3/12/96		12.0	0.79	0.28	1.60	0.37	na	1.16	7.47	7.17	6.43	1.0

na – data not available

measured in a separate mass spectrometer from neon, which was measured in a quadropole mass spectrometer. Details of the analytical procedures used for the helium isotope measurements are given in Ludin et al. (1997). Precision of the ^{4}He data is ±0.2 to 0.5%, that of the ^{3}He/^{4}He data is ±0.2 to 1%, and that of the neon data is ±0.5%. Greater scatter in the ^{4}He and neon concentrations can result from small air bubbles trapped in the copper tubes during sample collection.

Age dating with ^{3}H/^{3}He is done by calculating the amount of ^{3}He produced by the decay of ^{3}H since the water became isolated from the atmosphere (Clarke et al. 1976; Schlosser et al. 1988, 1989; Schlosser 1992). Details of the method for calculating tritiogenic ^{3}He are provided in Schlosser et al. (1989) and Solomon and Cook (2000). Most samples contained negligible amounts of helium from terrigenic sources, and an uncorrected ^{3}H/^{3}He age was reported. Four samples contained terrigenic helium and were corrected by assuming a radiogenic source, $R = 2 \times 10^{-8}$. This correction for terrigenic helium was significant only in samples from two wells (150 and 418). If dispersion is assumed negligible, then the age of a sample since it became isolated from the atmosphere can be calculated from the following equation:

$$\tau = T_{1/2}/\ln 2\ (1 + {}^3\mathrm{He}_{tri}/{}^3\mathrm{H}) \quad (1)$$

where τ is the ^{3}H/^{3}He age in years, $^3\mathrm{He}_{tri}$ is the tritiogenic ^{3}He concentration in TU, ^{3}H is the tritium concentration in TU, and $T_{1/2}$ is the ^{3}H half-life.

Modeling

Ground water and stream water samples were evaluated with NETPATH, a geochemical mass-balance model (Plummer et al. 1994), to determine whether unique combinations of chemical-weathering reactions could produce the measured changes in the concentrations of selected constituents. NETPATH reports every possible combination of specified geochemical reactions (called models here) that satisfy the constraints (chemical elements that must achieve mass balance) and plausible phases (minerals or other sources that may dissolve or precipitate). NETPATH alone cannot distinguish whether one model is more likely than another; thus, in the absence of additional information, all models must be considered equally likely. Samples were first corrected for evaporative concentration of chemical constituents based on the assumption that increases in Cl^- concentrations were entirely due to evapotranspiration; a similar assumption was made in an earlier study at PMRW (Peters and Ratcliffe 1998). The following phases were considered for possible dissolution: biotite, orthoclase feldspar, plagioclase feldspar (An_{23} and An_{32}), calcite, hornblende, and organic matter (CH_2O). The value of An_{23} for plagioclase is the mean composition reported in a recent weathering study at PMRW (White et al. 2001), and An_{32} is the mean value of the plagioclase in the amphibolite (Kelly 1987). Silica in the form of SiO_2 was considered for possible dissolution or precipitation within the riparian aquifer. Kaolinite, vermiculite, and CO_2 gas were considered for possible formation within the riparian aquifer. The

selection of these phases was based on previously reported mineralogical data from PMRW (Grant 1975; Nixon 1981; Kelly 1987; Shanley 1989; White et al. 2001). The constraints used to achieve mass balance included: calcium, magnesium, sodium, potassium, silicon, carbon, aluminum, chlorine, and redox state. The redox constraint assures that electrons are conserved in oxidation–reduction reactions. Only models that included formation of kaolinite were considered because kaolinite is the principal secondary mineral that forms through chemical weathering at PMRW.

Results and Discussion

This section discusses the ground water and surface water chemistry results, CFC and $^3H/^3He$ analyses for ground water age dating, results of the mass-balance modeling, calculation of chemical-weathering rates within the riparian aquifer, and presents a conceptual model of ground water flow and geochemical evolution.

Ground Water and Surface Water Chemistry

Concentrations of base cations, Cl^-, and SiO_2 in ground water generally increased downstream from the headwaters area to the gauge at the watershed outlet. The variability in ground water chemistry from well to well and with depth results from local variation in the geochemical and hydraulic factors that affect rates of chemical weathering and ground water transport. The highest concentrations were generally at the deepest well (150), which is nearest the outlet (Table 1). Concentrations of base cations and SiO_2 increased between fivefold and more than tenfold from the headwaters to the outlet, whereas Cl^- concentrations increased only about twofold. This difference is because base cation and SiO_2 concentrations increased through dissolution of aquifer minerals, whereas Cl^- concentrations increased mainly through evapotranspiration of ground water (little Cl^- is present in aquifer minerals). Solute concentrations in stream water at the outlet gauge were similar to those at many of the 300- and 400-series wells, midway down the watershed (see locations in Figure 1), whereas solute concentrations at the 10 ha gauge were similar to those of many of the 700- and 800-series wells, near the headwaters (Table 1).

Apparent Age of Ground Water

The apparent age of ground water at some wells differed depending on whether the age was derived from CFC–11, CFC–12, CFC–113, or $^3H/^3He$ (Tables 2 and 3). This discrepancy among the results of the age-dating methods in some instances was greater than an order of magnitude. Apparent age differences among the three CFC species in many wells were probably due to differential microbial degradation. Three of the 300-series wells (322, 323, and 324) had measurable concentrations of CH_4 accompanied by little or no (<0.1 mg/L) dissolved O_2. Eight other wells had concentrations of <5.0 mg/L dissolved O_2, suggesting some exposure to anaerobic conditions during transport (Table 4). Microbial degradation of CFCs has been demonstrated in natural environments and in laboratory experiments with natural materials, largely under anaerobic conditions (Lovley and Woodward 1992; Sonier et al. 1994; Deipser and Stegmann 1997). All three CFC species are potentially susceptible to microbial degradation, but CFC–11 is generally the most easily degraded (Oster et al. 1996; Plummer and Busenberg 2000). CFC–113 can adsorb to organic matter in soils and shallow ground water (Cook et al. 1995; Plummer and Busenberg 2000).

Concentrations of ^3H and ^3He are not susceptible to microbial degradation, but are affected by excess terrigenic helium or gas exchange at the water table. The effects of these processes on $^3H/^3He$ probably were minor compared to the effects of microbial degradation on CFCs, however; therefore, $^3H/^3He$-based age dates were compared with the CFC-based ages to assess which CFC ages were reliable. Results revealed that most of the CFC–11 and CFC–113–based apparent ages were biased high relative to those based on $^3H/^3He$ (Figure 2). Most CFC–12–based ages fell closer to the 1:1 line in Figure 2 than the CFC–11 and CFC–113–based ages, but were still biased high for wells 322, 323, and 324, that contain dissolved CH_4. Thus, all three CFC compounds became degraded by microbial processes in samples from methanogenic environments at PMRW. The apparent ages derived from CFC–12 agreed fairly well with those derived from $^3H/^3He$ for aerobic samples except for the sample from well 737, which was biased high for CFC–12. This sample had a low dissolved O_2 concentration of 2.6 mg/L, however (Table 4), and some of the CFC–12 in this sample may have been lost through sorption to soil organic matter, or in localized anaerobic zones in the soil or aquifer. Alternatively, the $^3H/^3He$-based age could have been too young due to gas exchange at the water table; this would affect CFCs as well, although to a lesser extent (Plummer et al. 2001).

The $^3H/^3He$ and CFC–12–based apparent ages in aerobic samples were assumed sufficiently reliable to use in additional analyses in this study, whereas the CFC–11 and CFC–113–based apparent ages were considered unreliable, and are not discussed further, nor were they used in any additional analyses in this study.

The apparent ages range from modern (≅0) to ~1.5 years for upstream wells (600, 700, and 800 series) to 26–27 years downstream at well 150 (Tables 2 and 3). Apparent ground water ages midway down the stream valley were

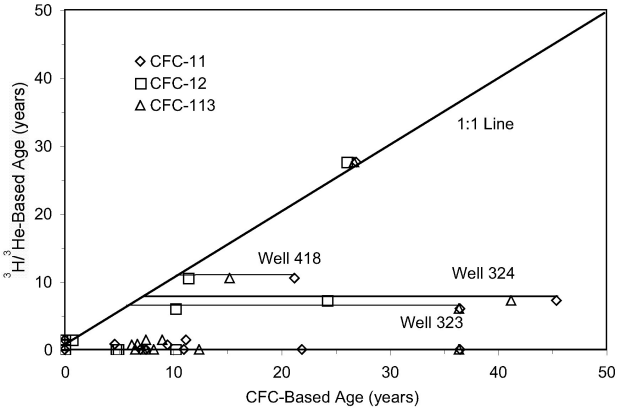

Figure 2. CFC- and $^3H/^3He$-based apparent ages of ground water at Panola Mountain Research Watershed, Georgia.

Table 2
CFC Concentrations, Calculated Atmospheric Mixing Ratios, and Apparent Ages of Ground Water and Surface Water at Panola Mountain Research Watershed, Georgia, March 1996, as Calculated from CFC Analyses

Sampling Site	CFC Concentration* (pg/kg)			Calculated Atmospheric Mixing Ratio (parts per trillion by volume)			Apparent CFC-Derived Age** (years)		
	CFC-11	CFC-12	CFC-113	CFC-11	CFC- 12	CFC-113	CFC-11	CFC-12	CFC-113
Wells									
130	251.9	216.9	40.1	120.5	439.9	47.8	21.0	**8.7**	10.7
150	127.8	72.7	5.4	54.8	133.8	5.7	**26.9**	**26.0**	**26.7**
285	678.2	374.1	101.7	216.3	528.2	77.0	11.0	**2.2**	6.2
316	284.3	299.5	44.7	99.2	458.0	37.4	22.7	**8.0**	12.4
322	32.8	280.2	2.3	10.9	411.8	1.8	36.5	10.2	>36.4
323	4.1	128.0	0.0	1.3	176.2	0.0	44.5	23.7	>41.2
324	2.8	118.8	0.0	0.9	164.4	0.0	45.4	24.2	>41.2
418	263.5	203.8	24.2	118.8	392.1	26.9	21.2	**11.4**	15.2
441	539.4	312.0	61.2	216.4	540.5	59.8	11.2	**0.7**	9.0
479	596.1	348.7	79.5	235.4	595.7	76.4	9.5	**0.0**	6.2
640	665.5	324.1	76.4	266.9	561.5	74.7	4.6	**0.0**	6.7
671.261	634.4	324.0	69.5	258.4	569.2	69.1	7.5	**0.0**	7.5
671.373	659.9	318.7	74.5	275.9	572.9	76.3	**0.0**	**0.0**	4.6
690	669.9	326.2	73.9	261.7	552.1	70.2	7.0	**0.0**	7.2
691	800.8	336.1	73.2	307.9	560.7	68.3	**0.0**	**0.0**	7.5
696	756.4	346.6	82.3	286.3	570.1	75.4	**0.0**	**0.0**	6.5
737	356.3	364.9	53.4	110.4	502.1	39.2	21.9	4.9	2.4
760	2624.1	346.3	81.4	915.3	529.6	68.1	**0.0**	**1.9**	7.5
801	618.9	329.7	77.0	217.1	506.7	64.8	11.0	**4.7**	8.2
821	810.9	372.4	83.1	276.7	558.4	67.8	**0.0**	**0.0**	7.7
Stream sites									
100	641.5	314.3	85.5	262.7	554.7	85.6	7.0	0.0	2.1
100	571.3	284.9	73.3	253.9	540.9	80.4	8.0	0.0	4.7

*Concentrations are mean values based on measurement of three replicate samples.
**Recharge temperatures for apparent-age calculations are given in Table 4. The most likely apparent ages for each sample are in boldface type; all other apparent ages are probably biased high through CFC degradation.

close to 0 at wells 441 and 479, 6 to 7 years at wells 323 and 324, and 10 to 11 years at well 418. These results suggest a general downstream increase in age. The apparent ages of ground water in wells 323 and 324 suggest that age also increases with depth in the riparian aquifer, and the data from well 150 (19.8 m deep) suggest that ground water that passes through fractures at depth in the granite is older than ground water in the overlying saprolite.

Relation of Apparent Age to Ground Water Chemistry

Strong positive correlations ($r^2 = 0.87–0.90$, $p < 0.001$, linear regression) were found between the apparent age of riparian ground water and SiO_2, Na^+, and Ca^{2+} concentrations (Figure 3). Strontium concentrations were also strongly related ($p < 0.001$) to the apparent age of riparian ground water, presumably reflecting a source from the weathering of plagioclase feldspar (relation not shown). The concentrations of Mg^{2+} were not strongly correlated with apparent ground water ages, which may reflect irregular contact during geochemical evolution with pods or lenses of amphibolite containing abundant hornblende and biotite. These correlations are consistent with (1) findings of a previous study at PMRW, wherein concentrations of these constituents increased with depth during vertical movement through the regolith on a ridgetop site (Stonestrom et al. 1998), (2) data from a recent study of springs of varying ages in terrain containing granodiorite and andesite in the Sierra Nevada (Rademacher et al. 2001), and (3) data from wells in fractured siliciclastics in the Valley and Ridge Province, Pennsylvania (Burton et al. 2002). These correlations at PMRW appear to be strongly leveraged by the data from well 150, but if these data are removed from the regression relations, the correlations for all three constituents remain highly significant ($p < 0.01$). The *y*-intercepts of these linear regression relations are 6.5 mg/L for SiO_2, 0.6 mg/L for Ca^{2+}, and 1.4 mg/L for Na^+, and can be inferred as mean values for recharge to the riparian aquifer.

The strong linear correlation between apparent age and the concentrations of these three solutes was used to estimate the mean age of base flow at the upper and downstream gauges. The mean ages range from 0.5 to 1.2 years for stream water at the upper gauge to 3.2 to 4.1 years at the downstream gauge, if piston flow and a constant rate of dissolution is assumed. Calculation of a mean age of base flow from these apparent age-solute relations is an approximation, however, because the age-frequency distribution of ground water discharging to the stream is unknown. For example, if ground water ages in a well-mixed reservoir are

Table 3

$^3H/^3He$ Data and Calculated Ages of Ground Water at Panola Mountain Research Watershed, Georgia, March 1996

Well	N_2–Ar Recharge Temp. (°C)	$^3H \pm (1\sigma)$ (TU)	δ^3He (%)	^4He (cc STP/g $\times 10^{-8}$)	Δ^4He (%)	Ne (cc STP/g $\times 10^{-7}$)	ΔNe (%)	He_{Terr} (% of Total He)	$^3H+^3He^*$ (Tritium Units)	Final $^3H/He$-Derived Age (Years)
150	13.6	14.3 (0.3)	34.22	11.47	157.6	2.44	28.5	47.6	66.4	27.6
150	13.6	14.4 (0.5)	35.52	11.45	157.2	2.47	30.2	46.7	66.7	27.5
322	9.0	19.2 (0.7)	–1.79	5.37	18.2	2.36	19.1	–4.9	17.7	–0.1
322	9.0	19.2 (0.7)	–1.86	5.42	19.5	2.37	19.7	–4.4	17.8	–0.1
323	7.6	16.9 (0.7)	20.33	5.49	20.3	2.38	18.4	–2.6	22.8	6.0
324	7.8	15.5 (0.6)	22.31	5.54	21.4	2.37	18.3	–1.5	22.4	6.9
324	7.8	15.5 (0.5)	24.77	5.53	21.2	2.37	18.1	–1.4	23.1	7.5
418	14.7	21.9 (0.8)	37.31	6.11	37.8	2.19	16.7	12.7	39.2	10.5
441	12.4	10.6 (0.5)	1.12	5.53	23.5	2.34	21.8	–2.7	10.5	1.3
441	12.4	10.6 (0.5)	1.38	5.47	22.3	2.34	22.0	–4.0	10.2	1.4
479	12.0	11.4 (0.2)	–0.42	6.25	39.4	2.61	35.6	–3.3	10.6	0.4
479	12.0	10.2 (0.5)	0.53	6.09	36.0	2.49	29.0	0.0	10.8	1.0
640	12.4	10.0 (0.5)	–0.34	6.17	38.0	2.51	31.0	–0.2	10.2	0.5
640	12.4	10.2 (0.2)	-0.57	6.21	38.9	2.50	30.3	1.0	10.8	1.0
671.261	12.7	10.5 (0.5)	–1.71	7.12	59.3	2.86	49.5	–1.1	9.8	–0.4
690	11.9	9.9 (0.2)	–2.18	5.66	26.3	2.33	20.8	0.4	9.8	–0.3
690	11.9	10.6 (0.5)	–1.45	5.80	29.5	2.44	26.8	–2.8	9.7	–0.1
691	11.6	10.3 (0.5)	–0.48	5.74	28.0	2.40	24.3	–1.7	10.0	0.5
691	11.6	9.1 (0.2)	–1.18	6.06	34.9	2.40	24.2	3.6	10.3	2.3
696	11.3	11.1 (0.5)	–2.01	5.01	11.5	2.17	12.0	–3.0	10.1	–0.2
737	7.7	8.1 (0.5)	–2.28	5.68	24.3	2.47	23.2	–4.1	6.5	–0.6
801	9.9	10.8 (0.7)	–1.70	5.43	20.2	2.29	16.6	–0.5	10.6	–0.1

Samples were not collected from wells 130, 285, 316, 671.373, 760, and 821.
Mean ages of duplicate samples were used in all other figures and calculations.
Recharge elevation was assumed to be 230 m above sea level.
Δ^4He and ΔNe are ^4He and Ne concentrations in excess of solubility equilibrium, reported in percent of solubility equilibrium.
$^3H+^3He^*$ is initial tritium expressed as ^3H + tritiogenic ^3He, reported in TU.
Final $^3H/^3He$ age was corrected for terrigenic helium, $R = 2 \times 10^{-8}$, if $^4He_{Terr} > 0\%$ of ^4He total.
Progagation of analytical precision leads to uncertainties of ± 0.2 years in the final age
STP, standard temperature and pressure

exponentially distributed (Maloszewski et al. 1992; Cook and Bohlke 2000), then the mean residence times of ground water discharging to the stream are 1.5 years at the upper gauge and 4.5 years at the downstream gauge. A recently published study suggests that a fractal model that is more complex than the exponential model is needed to describe the age distribution of stream water in small catchments (Kirchner et al. 2001); nevertheless, these values provide some estimates for the mean age of stream water.

Mass-Balance Modeling Results

Two scenarios of chemical evolution were examined. One represented ground water flowing along the entire valley length (~500 m) from the upstream wells to well 150, and the other represented flow from the upstream wells to the 300-series wells. The first scenario represents the greatest time for geochemical evolution that was measured in the riparian aquifer and bedrock, and the second potentially represents a different pathway of evolution because of the high Mg^{2+} concentrations per unit age in this part of the aquifer. The concentrations of dissolved solutes at the upstream wells were obtained from mean values of the 10 samples from the 600-, 700-, and 800-series wells, and the concentrations at the 300-series wells were obtained from the mean values of samples from three of those wells (316, 323, and 324).

Geochemical Evolution from the Upstream Wells to Well 150

NETPATH found eight models that produced mass balance and included the plausible phases that might dissolve or precipitate (Table 5). In all eight models, the principal weathering reaction was the dissolution of plagioclase feldspar and the formation of kaolinite; this is consistent with the findings of previous weathering studies at PMRW (Nixon 1981; Stonestrom et al. 1998; White et al. 2001). The dissolution of K-feldspar was present in five of eight models, and was the second most dominant dissolution reaction in two of those models; this is also consistent with

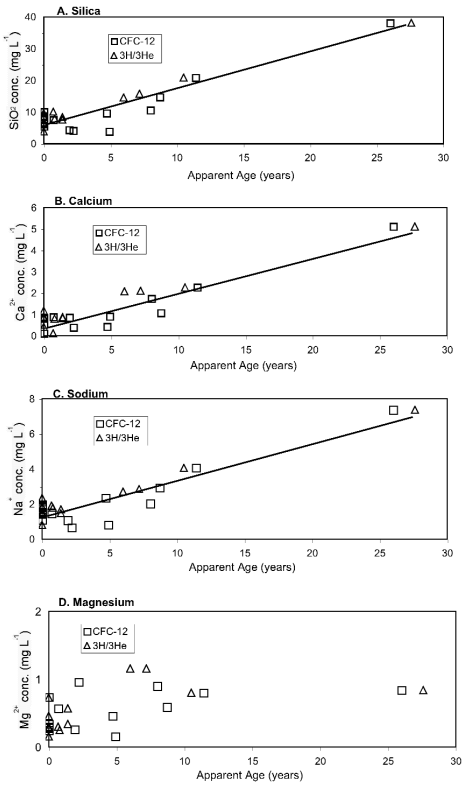

Figure 3. Concentrations of SiO_2, Ca^{2+}, Na^+, and Mg^{2+} in ground water at Panola Mountain Research Watershed, Georgia, as a function of apparent age calculated from CFC–12 and $^3H/^3He$ data. The graphs of SiO_2, Ca^{2+}, and Na^+ concentrations contain a best-fit linear regression line fit to all data.

the results of previous weathering studies at PMRW (Stonestrom et al. 1998; White et al. 2001).

In addition to feldspar weathering, five of the models include dissolution of biotite, and four include dissolution of hornblende, primarily to satisfy mass-balance constraints for Mg^{2+}. Biotite weathering has been identified as a slow but measurable process in the regolith at PMRW; thus, models that include biotite weathering are consistent with previous results in the watershed (White et al. 2002). Dissolution of hornblende is supported by results from a study in the nearby southern Blue Ridge, in which weathering of biotite and hornblende were necessary to explain the geochemical evolution of stream water in a watershed underlain by amphibolite, similar to that at PMRW (Velbel 1992). The present study ascribes only a minor role to amphibolite weathering, however, because most of the watershed is underlain by granite.

Three of the models also include the dissolution of calcite; this is consistent with the results of laboratory dissolution experiments that found initial dissolution of calcite in freshly exposed Panola Granite (White et al. 1999). The mass-balance modeling results suggest that ground water may have some contact with fresh granite from which calcite dissolves. Alternatively, calcite may have formed in the past from plagioclase weathering in the granite, and is now being dissolved.

Table 4

Dissolved Gas Concentrations, Recharge Temperatures, and Excess Air in Ground Water and Surface Water Samples from Panola Mountain Research Watershed, Georgia, March 1996

	Concentration (mg/L)					Recharge		Excess Air (cc STP/L)	
Well	N_2	Ar	O_2	CO_2	CH_4	Elevation (m Above Sea Level)	(°C)	N_2-Ar	Ne
130	15.13	0.5776	4.45	45.18	0.000	230	15.8	–0.6	nd
150	19.42	0.6675	6.83	40.50	0.000	230	13.6	3.1	3.1
285	20.87	0.7411	6.55	42.12	0.000	230	8.1	2.5	nd
316	19.06	0.6949	2.62	20.78	0.000	230	9.7	1.3	nd
322	20.32	0.7235	0.07	17.80	0.046	230	9.0	2.3	2.1
323	20.27	0.7358	0.02	34.72	0.643	230	7.6	1.6	2.0
324	20.00	0.7297	0.07	37.25	0.623	230	7.8	1.4	2.0
418	17.52	0.6269	0.34	56.61	0.000	230	14.7	1.5	1.7
441	19.20	0.6740	4.17	46.17	0.002	230	12.4	2.4	2.3
640	19.74	0.6830	4.71	36.12	0.000	30	12.4	3.0	3.2
671.261	19.16	0.6703	6.64	38.47	0.000	230	12.7	2.5	5.2*
671.373	17.59	0.6397	7.15	31.55	0.000	230	13.2	1.1	nd
690	18.95	0.6734	3.68	28.54	0.000	230	11.9	2.0	2.5
691	19.49	0.6855	3.63	32.15	0.000	230	11.6	2.4	2.6
696	18.36	0.6693	5.14	19.75	0.000	230	11.3	1.2	1.3
737	21.04	0.7486	2.62	37.92	0.000	230	7.7	2.4	2.6
760	18.99	0.6929	7.76	25.58	0.000	230	9.8	1.2	nd
801	18.87	0.6903	8.15	47.72	0.000	230	9.9	1.1	1.8
821	18.02	0.6801	7.47	35.63	0.000	230	9.4	0.1	nd

*Probable air leak
Data were not available for well 479
nd - not detected

Table 5

Range in Amount of Selected Phases That Would Have to Dissolve (+) or Precipitate (–) per Liter of Ground Water to Balance the Observed Increases in Concentrations of Seven Dissolved Constituents and Redox State in the Riparian Aquifer at Panola Mountain Research Watershed, March 1996, as Calculated for Two Scenarios of Geochemical Evolution

Phase	Number of Models That Include Phase	Range in Amount Dissolved or Precipated, in µmol/L* Ground Water
Scenario 1 – Upstream Wells to Well 150	Total Models = 8	
Plagioclase (An_{23})	8	+1.9 to +166.8
Kaolinite	8	–105.6 to –127.0
Organic matter	8	+52.5 to +69.2
Carbon dioxide gas	8	–23.3 to –49.2
Silica	8	–5.4 to –53.9
Biotite	5	+4.6 to +12.3
K-feldspar	5	+5.2 to +10.9
Hornblende	4	+6.9 to +21.9
Vermiculite	4	–2.9 to –11.1
Calcite	3	+14.5 to +21.5
Plagioclase (An_{32})	3	+124.0 to +184.2
Scenario 2 – Upstream Wells to 300-Series Wells	Total Models = 4	
Plagioclase (An_{23})	4	+22.7 to +23.9
Kaolinite	4	–24.0 to –24.1
Biotite	4	+3.8 to +3.9
Carbon dioxide gas	4	–256.4 to –256.6
Hornblende	4	+14.7 to +14.8
Organic matter	4	+207.4 to +207.5
Silica	4	–19.7 to –20.1
Calcite	1	+0.1
K-feldspar	1	+0.1
Plagioclase (An_{32})	1	+1.3
Vermiculite	1	–0.1

Calculations were done with the NETPATH model.
*Concentrations of all constituents were adjusted on assumption that the increase in Cl^- concentration was due to evaporation.

Geochemical Evolution from the Upstream Wells to the 300-Series Wells

Model results for geochemical evolution from the upstream wells to the 300 series are similar to those for evolution to well 150, except that a greater role was found for the weathering of biotite and hornblende in this scenario (Table 5). A sharp rise in Mg^{2+} concentrations in stream water—an indication of amphibolite weathering—has been noted in the area near the 300-series wells (N.E. Peters, unpublished data). Ground water samples from the 300-series wells also have greater Mg^{2+} concentrations for their apparent ages than ground water from wells 130 or 150 farther downstream (Figure 3d). All four models that describe geochemical evolution of ground water at the 300-series wells include weathering of biotite and hornblende. The amount of hornblende weathering in these models represents a greater proportion of the total weathering than was observed in the mass-balance models for evolution to well 150. Only one model includes the dissolution of K-feldspar, an indication of less weathering of this mineral in the upstream part of the aquifer than farther downstream. The reason for this difference is unknown; however, cation-exchange reactions or biological uptake may have decreased K^+ concentrations in the upstream part of the aquifer, which would result in less apparent weathering of K-feldspar.

One of the models includes the weathering of the more calcic of the modeled plagioclase (An_{32}) during geochemical evolution from the upper wells to the 300-series wells; weathering of An_{32} is also supported by a shift of the sodium/calcium molar ratio from ~3.8, typical of weathering of plagioclase with a composition of $An_{20–25}$, to a value of ~2.3, close to that expected by weathering of An_{32}. As stated previously, however, a range of plagioclase compositions may be present in the watershed, and additionally, the weathering of calcite or cation exchange may have affected Ca^{2+} concentrations to produce a similar shift in the sodium/calcium ratio.

Chemical Weathering Rates

Chemical weathering rates in mass per liter of ground water were calculated for the same two scenarios of geochemical evolution discussed previously: (1) upper wells to well 150, and (2) upper wells to 300-series wells. The elapsed time used in these weathering rate calculations based on the apparent age differences obtained by CFC–12

and $^3H/^3He$ age-dating techniques was 26 years for scenario 1, and 6.5 years for scenario 2.

The greatest weathering rates were those for plagioclase feldspar—6.3 to 7.2 µmol/L/year for scenario 1, and 3.7 µmol/L/year for scenario 2 (Table 6). The higher rates obtained for scenario 1 may reflect the inclusion of well 150, which is finished in granite. Thus, at least some part of the transit time was in bedrock fractures, where weathering rates may be more rapid than in the saprolite in which the other wells are finished. The weathering rates obtained for these two scenarios are consistent with those measured by Rademacher et al. (2001) in springs of the Sierra Nevada (3.6 to 11.6 µmol/L/year) through a method similar to the one employed in this study.

The mineral whose weathering rate varied most widely was K-feldspar—from 0.015 µmol/L/year in scenario 2 to 0.42 µmol/L/year in one of the models of scenario 1 (Table 6). In general, the weathering rate of K-feldspar was 10 to 30 times lower than that of plagioclase, and K-feldspar weathering was present in only six of the 12 possible models provided by NETPATH. In contrast, the weathering rate of K-feldspar calculated at PMRW by White et al. (2001) was only two to three times lower than the rate for plagioclase weathering.

The weathering rates of the mafic minerals in both scenarios ranged from 0.27 to 2.3 µmol/L/year for hornblende and 0.18 to 0.60 µmol/L/year for biotite (Table 6). The weathering rate for hornblende is similar to the values of 0.6 to 1.8 µmol/L/year reported by Rademacher et al. (2001) for the Sierra Nevada. The weathering rate calculated for biotite during the current study is consistent with a previously calculated weathering rate for biotite at PMRW that is approximately one order of magnitude less than that of plagioclase (White et al. 2002).

To compare the chemical weathering rates calculated in this study with most of those reported in the literature (with the exception of Rademacher et al. 2001), data on the mineral-surface area are required. The units of dissolution rate (µmol/L/year) used in this study were adopted because the riparian aquifer is unconfined; even if estimates of the porosity, mineral-surface area, bulk density, and dimensions of the riparian aquifer were used, the mineral-surface area with which ground water has been in contact before entering this aquifer laterally from the adjacent hillslopes is unknown.

Alternatively, the in situ weathering rate for plagioclase at PMRW calculated by White et al. (2001) can be used to estimate the amount of mineral-surface area to which water had to have been exposed to yield the rates obtained in this study. The plagioclase-weathering rate calculated by White et al. (2001) for saprolite at a ridgetop site at PMRW is 8.8×10^{-3} µmol/m^2/year. Using a plagioclase-weathering rate of 6.4 µmol/L/year from this study indicates that 1 L of riparian ground water would have had to contact ~730 m^2 of plagioclase surface area in a year for the two rates to be equivalent. Assuming the specific surface area of weathered feldspars in granites is 1 m^2/g and that saprolite at a depth of ~2 m is 15% plagioclase (White et al. 2001), ground water would have to contact ~4900 g of saprolite. If a bulk density of 1.4 g/cm^3 is assumed (value at 1.85 m depth in saprolite, Stonestrom et al. 1998), this liter of ground water would have to contact ~3500 cm^3 of aquifer material during the year to equal the weathering rate obtained by White et al. (2001). One liter of ground water within the Panola riparian aquifer (porosity ~0.5, Stonestrom et al. 1998) occupies 2000 cm^3 (12.5 cm × 12.5 cm × 12.5 cm). If the saturated hydraulic conductivity of the riparian aquifer is 8.8×10^{-6} cm/sec (reported for a depth of 1.85 m at a ridgetop site in saprolite at PMRW by Stonestrom et al. 1998), the liter of water would move ~22 cm/year on a 4% gradient (slope of the riparian aquifer surface) according to Darcy's law. This is equivalent to ~3400 cm^3 of aquifer material for 1 L of water that passes through a volume of 12.5 cm × 12.5 cm × 22 cm in one year. This estimate of 3400 cm^3 is essentially equivalent to the 3500 cm^3 of aquifer material necessary to produce the plagioclase-weathering rate of White et al. (2001) and, thus, suggests that the rate of plagioclase weathering calculated in

Table 6
Mineral-Weathering Rates Calculated for Five Models for Two Scenarios of Geochemical Evolution in the Riparian Aquifer at Panola Mountain Research Watershed, Georgia, March 1996

Mineral Phase	Number of Models That Include Phase	Median Mineral Weathering Rate, in µmol L/yr	Range in Mineral Weathering Rate, in µmol L/yr
Scenario 1 – Upstream Wells to Well 150	Total Models = 8		
Plagioclase (total)	8	6.4	6.3 – 7.2
Biotite	5	0.40	0.18 – 0.47
K-feldspar	5	0.29	0.20 – 0.42
Hornblende	4	0.55	0.27 – 0.84
Calcite	3	0.82	0.56 – 0.83
Scenario 2 – Upstream Wells to 300-Series Wells	Total Models = 4		
Plagioclase (total)	4	3.7	3.7
Biotite	4	0.60	0.58 – 0.60
Hornblende	4	2.3	2.3
K-feldspar	1	0.015	0.015

Rates based on 26 years for scenario 1 and 6.5 years for scenario 2

this study is similar to the rate calculated by White et al. (2001). The plagioclase-weathering rate of White et al. (2001) is three to four orders of magnitude lower than that derived from experimental dissolution of plagioclase in the laboratory (Busenberg and Clemency 1976; Knauss and Wolery 1986; Oxburgh et al. 1994); therefore, the rate calculated in this study is similarly three to four orders of magnitude less than the laboratory-derived rates. Further confirmation of the similarity in feldspar weathering rates of this study with that of White et al. (2001) will require detailed study of transport rates and mineral-surface area in the riparian aquifer.

Conceptual Model of Ground Water Flow and Geochemical Evolution

The spatial patterns of apparent age and geochemical evolution of riparian ground water determined in this study, when combined with the results of previous hydrologic and geochemical studies at PMRW (Burns et al. 1998; Hooper et al. 1998; Peters and Ratcliffe 1998; Burns et al. 2001; Freer et al. 2002), provide the basis for a conceptual model of ground water flow and geochemical evolution at PMRW with the following components: (1) large amounts of aquifer recharge from headwater hillslopes and the granite outcrop by young water that moves slowly down the stream valley, (2) small amounts of continued recharge downstream along the valley from the surface and adjacent hillslopes, and (3) small downstream contributions from deeper ground water that has previously been exposed to weathering of the underlying amphibolite and granodiorite. This conceptual model implies that the riparian aquifer is a semi-open ground water flow system that receives only small contributions of ground water from adjacent hillslopes and from the underlying bedrock. Previous results have shown that most subsurface stormflow from adjacent hillslopes transits rapidly through the uppermost part of the riparian aquifer, although some remains as fresh recharge after storms (Burns et al. 2001).

The sharp increases in Mg^{2+} concentrations and in hornblende/biotite weathering in the 300-series wells suggest a contribution midway down the valley of deeper ground water that has been exposed to amphibolite weathering. Results from the mass-balance models also indicate the possibility of calcite weathering, which suggests a contribution of deeper ground water that has been exposed to fresh granodiorite. Alternatively, the results of the two modeling scenarios could suggest two pathways of chemical evolution—one with a large Mg^{2+}/hornblende/biotite influence midvalley, and another with greater plagioclase/K-feldspar influence downstream near the catchment outlet. Both pathways of chemical evolution are probably controlled by the locations and depths of amphibolite and granodiorite relative to the principal pathways of ground water movement. One unanswered question relates to the pathway of hydrologic and geochemical evolution in the riparian saprolite from midvalley (the 300- and 400-series wells) to near the catchment outlet (well 130). The concentrations of Mg^{2+} are higher in wells 323, 324, and 418 than in well 130, and the apparent ages of ground water in these wells are similar to or greater than in well 130. This suggests a contribution from young ground water with low Mg^{2+} concentrations along this lower part of the stream valley. This contribution could be ground water from the two tributary valleys that enter the main valley between the 300- and 400-series wells and well 130. Additional sampling of ground water along this lower part of the valley would be needed to reveal the cause of the observed patterns of ground water geochemical evolution.

Summary and Conclusions

Ground water from 19 shallow wells screened in saprolite and one borehole finished in granite at the 41 ha PMRW generally show a downstream increase in concentrations of base cations and silica from the headwaters to the outlet. Age dating of this ground water through CFC and $^3H/^3He$ analysis indicates that many of the apparent ages calculated from CFC–11 and CFC–113 are too high, probably due to microbial degradation in anoxic and suboxic waters. Most of the CFC–12–derived ages match the $^3H/^3He$ ages fairly well, except for samples from three wells with measurable CH_4 concentrations; this indicates even CFC–12 can undergo degradation in methanogenic conditions.

The valid apparent ages were strongly correlated with concentrations of SiO_2, Na^+, and Ca^{2+} in the ground water, an indication of steady rates of chemical weathering of silicate minerals contained in the saprolite derived from the weathering of granite and amphibolite. These correlations between ground water age and chemistry were used to calculate a mean residence time of stream base flow of 1.5 years at the 10 ha midvalley gauge and 4.5 years at the 41 ha outlet gauge.

The NETPATH modeling results indicate that the dominant weathering reactant during geochemical evolution in the riparian aquifer is plagioclase feldspar, and that, additionally, contributions from the weathering of K-feldspar, hornblende, biotite, and calcite may be necessary to achieve mass balance. Plagioclase had the fastest weathering rate (~6.4 μmol/L/year) of any of the silicate minerals studied—a value that is comparable to results from a recent study of weathering rates in springs of the Sierra Nevada that used methods similar to those used in this study. Weathering rates calculated for K-feldspar, biotite, and hornblende ranged from three to 30 times lower than those of plagioclase. These calculated weathering rates cannot be converted to units of per-mineral surface area used in most weathering studies, however, because the riparian aquifer is unconfined and receives contributions from adjacent hillslopes in which the mineral surface area that is in contact with water cannot be estimated. Nevertheless, an estimate of the mineral-surface area to which 1 L of riparian ground water would be exposed during a year provided a plagioclase-weathering rate that was equivalent to that reported for saprolite at a nearby ridgetop site at PMRW. Further study of transport rates and mineral-surface area within the riparian aquifer are necessary to confirm the estimates derived in this study.

The results of this study indicate that modeling the geochemical evolution of base cations and silica within the riparian aquifer requires principally (if not solely) the weathering of silicate minerals; cation-exchange reactions

cannot be excluded, but are not necessary to achieve mass balance during geochemical evolution. This contrasts with the chemical evolution of subsurface flow on a hillslope at PMRW, in which fast cation-exchange reactions are hypothesized to be the principal source of base cations (Burns et al. 1998). Because riparian ground water is the predominant source of base flow at PMRW, and also is a large component of stormflow (Burns et al. 2001), successful predictive models of the future effects of acid precipitation and climate change on stream water chemistry should include these weathering reactions.

Acknowledgments

This research was supported by a grant from the National Science Foundation (EAR940253) and was conducted in cooperation with the Georgia Department of Natural Resources. The authors thank Brent Aulenbach, Ed Drake (deceased), Hannah Green, and Ho Joong Youn for their assistance with this investigation. Alex Blum and Tom Bullen provided thoughtful reviews of an earlier version of this manuscript, and Scott Bailey, David Stonestrom, and an anonymous reviewer provided helpful reviews of the manuscript version first submitted to the journal.

Author's Note: Use of brands names is for identification purposes only, and does not constitute endorsement by the U.S. Government.

Editor's Note: The use of brand names in peer-reviewed papers is for identification purposes only and does not constitute endorsement by the authors, their employers, or the National Ground Water Association.

References

Atkins, R.L., and M.W. Higgins. 1980. Superimposed folding and its bearing on geologic history of the Atlanta, Georgia area. In *Excursions in Southeastern Geology*, vol. 1, ed. R.W. Frey, 19–40. Alexandria, Virginia: American Geological Institute.

Bishop, K.H., H. Grip, and A. O'Neill. 1990. The origins of acid runoff in a hillslope during storm events. *Journal of Hydrology* 116, 35–61.

Bu, X., and M.J. Warner. 1995. Solubility of chlorofluorocarbon 113 in water and seawater. *Deep-Sea Research* 42, 1151–1161.

Burns, D.A., R.P. Hooper, J.J. McDonnell, J.E. Freer, C. Kendall, and K. Beven. 1998. Base cation concentrations in subsurface flow from a forested hillslope: The role of flushing frequency. *Water Resources Research* 34, 3535–3544.

Burns, D.A., R.P. Hooper, J.J. McDonnell, N.E. Peters, J.E. Freer, C. Kendall, and K. Beven. 2001. Quantifying contributions to storm runoff using end-member mixing analysis and hydrologic measurements at the Panola Mountain Research Watershed (Georgia, USA). *Hydrological Processes* 15, 1903–1924.

Burton, W.C., L.N. Plummer, E. Busenberg, B.D. Lindsey, and W.J. Gburek. 2002. Influence of fracture anisotropy on ground water ages and chemistry, Valley and Ridge Province, Pennsylvania. *Ground Water* 40, no. 3: 242–257.

Busenberg, E., and C.V. Clemency. 1976. The dissolution kinetics of feldspars at 25°C and 1 atm CO_2 partial pressure. *Geochimica et Cosmochimica Acta* 40, 41–49.

Busenberg, E., and L.N. Plummer. 1992. Use of chlorofluoromethanes (CCl_3F and CCl_2F_2) as hydrologic tracers and age-dating tools: Example. The alluvium and terrace system of central Oklahoma. *Water Resources Research* 28, 2257–2283.

Carter, M.E.B. 1978. A community analysis of the Piedmont deciduous forest of Panola Mountain Conservation Park: Atlanta, Georgia. M.S. thesis, Department of Biology, Emory University, Atlanta, Georgia.

Carter, R.F., and H.R. Stiles. 1983. Average annual rainfall and runoff in Georgia, 1941–70. Georgia Geologic Survey, *Hydrologic Atlas 9*, 1 sheet.

Clarke, W.B., W.J. Jenkins, and Z. Top. 1976. Determination of tritium by mass spectrometric measurement of ^{3}He. *International Journal of Applied Radiation and Isotopes* 27, 515–522.

Cook, P.G., and J.K. Bohlke. 2000. Determining timescales for groundwater flow and solute transport. In *Environmental Tracers in Subsurface Hydrology*, Chapter 1, ed. P.G. Cook and A. Herzeg, 1–30. Boston: Kluwer Academic Press.

Cook, P.G., D.K. Solomon, L.N. Plummer, E. Busenberg, and S.L. Schiff. 1995. Chlorofluorocarbons as tracers of groundwater transport processes in a shallow, silty sand aquifer. *Water Resources Research* 31, 425–434.

Cosby, B.J., R.F. Wright, G.M. Hornberger, and J.N. Galloway. 1985. Modeling the effects of acid deposition: Assessment of a lumped parameter model of soil water and stream water chemistry. *Water Resources Research* 21, 51–63.

Deipser, A., and R. Stegmann. 1997. Biological degradation of VCCs and CFCs under simulated landfill conditions in laboratory test digesters. *Environmental Science and Pollution Research International* 4, 209–216.

Freer, J., J.J. McDonnell, K.J. Beven, N.E. Peters, D.A. Burns, R.P. Hooper, B. Aulenbach, and C. Kendall. 2002. The role of bedrock topography on subsurface storm flow. *Water Resources Research* 38, no. 12: doi: 10.1029/ 2001WR000872.

Gillham, R.W., and C.J Jayatilaka. 1998. Response to Comment by Jeffrey J. McDonnell and James M. Buttle on "A deterministic-empirical model of the effect of the capillary-fringe on near-stream runoff. 1. Description of the model" (*Journal of Hydrology* 184 (1996) 299–315). *Journal of Hydrology* 207, 286–289.

Grant, W.H. 1975. Chemical weathering of Panola adamellite with special reference to apatite. *Southeastern Geology* 17, 17–58.

Heaton, T.H.E. 1981. Dissolved gases: Some applications to groundwater research. *Transactions of the Geological Society of South Africa* 84, 91–97.

Heaton, T.H.E., and J.C. Vogel. 1981. "Excess air" in groundwater. *Journal of Hydrology* 50, 201–216.

Higgins, M.W., R.L. Atkins, T.J. Crawford, R.F. Crawford III, R. Brooks, and R.B. Cook. 1988. The structure, stratigraphy, technostratigraphy, and evolution of the southernmost part of the Appalachian Orogen. U.S. Geological Survey Professional Paper 1475.

Hooper R.P., B.T. Aulenbach, D.A. Burns, J. McDonnell, J. Freer, C. Kendall, and K. Beven. 1998. Riparian control of streamwater chemistry: Implications for hydrochemical basin models. In *Hydrology, Water Resources and Ecology in Headwater,* ed. K. Kovar, U. Tappeiner, N.E. Peters, and R.G. Craig. IAHS Publication 248, 451–458. Wallingford, Oxon, U.K.: International Association of Hydrological Sciences.

Huntington, T.G., R.P. Hooper, N.E. Peters, T.D. Bullen, and C. Kendall. 1993. Water, energy, and biogeochemical budgets investigation at Panola Mountain Research Watershed, Stockbridge, Georgia: A research plan. U.S. Geological Survey Open-File Report 93–55.

Jayatilaka, C.J., and R.W. Gillham. 1996. A deterministic-empirical model of the effect of the capillary-fringe on near-stream area runoff, I: Description of the model. *Journal of Hydrology* 184, 299–315.

Johnson, D.W., and S.E. Lindberg (eds.). 1992. *Atmospheric Deposition and Forest Nutrient Cycling: A Synthesis of the Integrated Forest Study*. Ecological Studies 91. New York: Springer-Verlag.

Kelly, W.M. 1987. Personal communication via written memo to N.E. Peters.

Kirchner, J.W., X. Feng, and C. Neal. 2001. Catchment-scale advection and dispersion as a mechanism for fractal scaling in stream tracer concentrations. *Journal of Hydrology* 254, 82–101.

Knauss, K.G., and T.J. Wolery. 1986. Dependence of albite dissolution kinetics on pH and time at 25°C and 70°C. *Geochimica et Cosmochimica Acta* 50, 2481–2497.

Lovley, D.R., and J.C. Woodward. 1992. Consumption of Freons and CFC–11 and CFC–12 by anaerobic sediments and soils. *Environmental Science and Technology* 26, 925–929.

Ludin, A., R. Weppernig, G. Boenisch, and P. Schlosser. 1997. Mass spectrometric measurement of helium isotopes and tritium. Palisades, New York: Lamont-Doherty Earth Observatory.

Maloszewski, P., W. Rauert, P. Trimborn, A. Hermann, and R. Rau. 1992. Isotope hydrological study of mean transit times in an alpine basin (Wimbachtal, Germany). *Journal of Hydrology* 140, 343–360.

McDonnell, J.J., and J.M. Buttle. 1998. Comment on "A deterministic-empirical model of the effect of the capillary-fringe on near-stream runoff, I: Description of the model" by C.J. Jayatilaka and R.W. Gillham. *Journal of Hydrology* 207, 280–285.

Nixon, R.A. 1981. Rates and mechanisms of chemical weathering in an organic environment at Panola Mountain, Georgia. Ph.D. dissertation, Department of Geology, Emory University, Atlanta, Georgia.

National Oceanic and Atmospheric Administration. 1991. Local climatological data, annual summary with comparative data, 1990, Atlanta, Georgia. Asheville, North Carolina: NOAA.

Oster, H., C. Sonntag, and K.O. Munnich, 1996. Groundwater age dating with chlorofluorocarbons. *Water Resources Research* 32, 2989–3001.

Oxburgh, R., J.L. Drever, and Y.T. Sun. 1994. Mechanism of plagioclase dissolution in acid solutions at 25°C. *Geochimica et Cosmochimica Acta* 58, 661–669.

Peters, N.E., and E.B Ratcliffe. 1998. Tracing hydrologic pathways using chloride at the Panola Mountain Research Watershed, Georgia, USA. *Water, Air, and Soil Pollution* 105, 263–275.

Plummer, L.N., and E. Busenberg. 2000. Chlorofluorocarbons. In *Environmental Tracers in Subsurface Hydrology*, ed. P.G. Cook and A. L. Herczeg, 441–478. Boston: Kluwer Academic Publishers.

Plummer, L.N., E.C. Prestemon, and D.L. Parkhurst. 1994. An interactive code (NETPATH) for modeling net geochemical reactions along a flow path, version 2.0. U.S. Geological Survey Water-Resources Investigations 94–4169.

Plummer, L.N., E. Busenberg, J.K. Bohlke, D.L. Nelms, R.L. Michel, and P. Schlosser. 2001. Groundwater residence times in Shenandoah National Park, Blue Ridge Mountains, Virginia, USA: A multi-tracer approach. *Chemical Geology* 179, 93–111.

Rademacher, L.K., J.F. Clark, G.B. Hudson, D.C. Erman, and N.A. Erman. 2001. Chemical evolution of shallow groundwater as recorded by springs, Sagehen basin; Nevada County, California. *Chemical Geology* 179, 37–51.

Reuss, J.O., and D.W. Johnson. 1986. Acid deposition and the acidification of soils and waters. *Ecological Studies 59*. New York: Springer-Verlag.

Robson, A., K. Beven, and C. Neal. 1992. Towards identifying sources of subsurface flow: A comparison of components identified by a physically based runoff model and those determined by chemical mixing techniques. *Hydrologic Processes* 6, 199–214.

Schlosser, P. 1992. Tritium/^{3}He dating of waters in natural systems. In *Isotopes of Noble Gases as Tracers in Environmental Studies*. Vienna International Atomic Energy Agency.

Schlosser, P., M. Stute, H. Dorr, C. Sonntag, and K.O. Munnich. 1988. Tritium/^{3}He dating of shallow groundwater. *Earth and Planetary Science Letters* 89, 353–362.

Schlosser, P., M. Stute, C. Sonntag, and K.O. Munnich. 1989. Tritiogenic ^{3}He in shallow groundwater. *Earth and Planetary Science Letters* 94, 245–256.

Shanley, J.B. 1989. Factors controlling sulfate retention and transport at Panola Mountain, Georgia. Ph.D. dissertation, Department of Geology, University of Wyoming, Laramie.

Solomon, D.K., and P.G. Cook. 2000. ^{3}H and ^{3}He. In *Environmental Tracers in Subsurface Hydrology*, ed. P.G. Cook and A. L. Herczeg, 397–424. Boston: Kluwer Academic Publishers.

Sonier, D.N., N.L. Duran, and G.B. Smith. 1994. Dechlorination of trichlorofluoromethane (CFC–11) by sulfate-reducing bacteria from an aquifer contaminated with halogenated aliphatic compounds. *Applied Environmental Microbiology* 60, 4567–4572.

Stonestrom, D.A., A.F White, and K.C. Akstin. 1998. Determining rates of chemical weathering in soils—Solute transport versus profile evolution. *Journal of Hydrology* 209, 331–345.

Turton, D.J., C.T. Haan, and E.L. Miller. 1992. Subsurface flow responses of a small forested catchment in the Ouachita Mountains. *Hydrologic Processes* 6, 111–125.

Velbel, M.A. 1992. Geochemical mass balances and weathering rates in forested watersheds of the southern Blue Ridge, III: Cation budgets and the weathering rate of amphibole. *American Journal of Science* 292, 58–78.

Warner, M.J., and R.F. Weiss. 1985. Solubilities of chlorofluorcarbons 11 and 12 in water and seawater. *Deep Sea Research* 32, 1485–1497.

Wheater, H.S., S.J. Langan, A. Brown, and M.B. Beck. 1991. Hydrological response of the Allt A'Mharcaidh catchment—Inferences from experimental plots. *Journal of Hydrology* 123, 163–199.

White, A.F., T.D. Bullen, D.V. Vivit, M.S. Schulz, and D.W. Clow. 1999. The role of disseminated calcite in the chemical weathering of granitoid rocks. *Geochimica et Cosmochimica Acta* 63, 1939–1953.

White, A. F., T.D. Bullen, M.S. Schulz, A.E. Blum, T.G. Huntington, and N.E. Peters. 2001. Differential rates of feldspar weathering in granitic regoliths. *Geochimica et Cosmochimica Acta* 65, 847–869.

White, A.F., A.E. Blum, M.S. Shulz, T.G. Huntington, N.E. Peters, and D.A. Stonestrom. 2002. Chemical weathering of the Panola Granite: Solute and regolith elemental fluxes and the weathering rate of biotite. In *Water Rock Interactions, Ore Deposits, and Environmental Geochemistry: A Tribute to David A. Crerar*, ed. R. Hellmann and S.A. Wood. Geochemical Society Special Publication 7, 37–59. St. Louis, Missouri: Geochemical Society.

Zumbuhl, A.J. 1999. The relationship between soil depth and terrain attributes in a headwater Piedmont catchment. M.S. thesis, College of Environmental Science and Forestry, State University of New York, Syracuse, New York.